CHAPTER 7

Analysis of Pre-Cardiac MESP1 Progenitor Proliferation at Single Cell Level using an eGFP-Anillin Reporter Line

Sabine C. den Hartogh[1], Lu Cao[1], Tom Zwetsloot[1], Alexandra Raulf[2], Aniek van Wijngaarden[1], Michael Hesse[2], Bernd K. Fleischmann[2], Christine Mummery[1], Robert Passier[1,3].

1. Leiden University Medical Center, Dept. Anatomy and Embryology, Leiden, The Netherlands.
2. Institute of Physiology I, Life and Brain Center, University of Bonn, 53105 Bonn, Germany.
3. Department of Applied Stem cell Technologies. MIRA Institute for Biomedical Technology and Technical Medicine. University of Twente, P.O.Box 217, Enschede, The Netherlands.

ABSTRACT

Production of cardiomyocytes from human pluripotent stem cells (PSCs) provides not only promising opportunities for both *in vitro* as well as *in vivo* translational applications, but also may lead to a better understanding of signalling pathways and biological processes during the early phases of cardiac differentiation and development. For translational applications in drug development, disease modelling and cell-based therapy, it is important to obtain a large amount of highly purified cardiomyocytes from PSCs. Alternatively, controlled and defined expansion of cardiac progenitor cells offers additional advantages. Here, we studied the proliferative capacity of pre-cardiac MESP1 progenitors through the combinatorial use of fluorescent proliferation reporter eGFP-Anillin and the previously generated MESP1-mCherry cardiac reporter line. Scaffolding protein anillin is localized at distinct locations during the cell cycle, and fusion to eGFP enables distinction from cytokinesis with other cell cycle stages. It is currently unknown what the proliferative capacity is of MESP-positive pre-cardiac progenitors and how they respond to changes in environmental conditions. Therefore, we studied the proliferative capacity by analysis of subcellular localization of eGFP-Anillin in MESP1-mCherry progenitors under controlled culture conditions and using time-lapse microscopy. In addition, we screened several small molecules and growth factors on the ability to enhance MESP1 progenitor proliferation.

INTRODUCTION

Heart disease is the most common cause of death in most Western societies, unlocking the potential of regenerative stem cell- and drug therapy[1]. For successful development of cell-based therapies, large numbers of human cardiac cells will be necessary. Human pluripotent stem cells (hPSCs) can be efficiently differentiated to cardiac cells[2, 3], however, the inverse relationship between the degree of differentiation and the proliferation rate of cardiomyocytes limits the production of cardiac cells and advocates striving for an expandable cardiac progenitor population. When hPSCs, including induced PSCs (hiPSCs) and embryonic SCs (hESCs), differentiate towards the cardiac cells they first transit from a mesendodermal stage, expressing genes such as Brachyury T, MIXL1, and Eomesodermin, to a pre-cardiac mesodermal stage, marked by the expression of transcription factor MESP1[4]. These cells then further segregate to distinct multi-potent cardiac progenitor cells (CPCs), and start to express cardiac transcription factor NKX2-5[5]. These CPCs are capable of further differentiation into several cardiac cell subtypes, including atrial, ventricular, pacemaker-like cardiomyocytes, but also endothelial, and smooth muscle cells. In order to obtain high yields of cardiac subtype populations and to control maintenance and expansion of CPCs, it is of interest to understand the underlying mechanisms[6-9]. Several studies have demonstrated a crucial role for FGF-, IGF-, Notch1, and Wnt/B-catenin signaling pathways for self-renewal/expansion of CPCs. Nevertheless, the self-renewing capacity of specific CPCs and their biological responses may vary between different CPCs and/or developmental stages. As we know from *in vivo* studies in mice, almost all cells of the heart are derived from MESP1 expressing progenitors[10]. Therefore, it is for both regenerative and drug development studies of interest to understand whether we are able to maintain and expand human MESP1 progenitors in culture.

In order to study the proliferative capacity of MESP1 progenitors, we made use of a *in vivo* reporter system using the scaffolding protein anillin fused to enhanced green fluorescent protein (eGFP), to provide high spatiotemporal resolution of the mitotic phase[11]. Anillin is localized at specific subcellular locations in the cell during cytokinesis and midbody formation, enabling a clear visual separation of the different phases of the cell cycle, including cell division (**Fig 1**). Anillin is localized in the cell nucleus during G1-phase, S-phase, and G2-phase, and moves to the cytoplasm when entering the M-phase. Prior to cell division, anillin locates in the cytoskeleton ring and becomes restricted to the midbody region upon cytokinesis. When cells leave an active cell cycle, anillin gets degraded.

Here, we generated a dual fluorescent reporter line by introducing eGFP-Anillin in the MESP1$^{w/mCherry}$ hESC line, allowing live imaging of the different phases of cell division of cardiac progenitors and their derivatives[11]. Using time-lapse microscopy we were able to visualize the dynamics of MESP1-expressing progenitors. We measured a low proliferative capacity of these progenitors during *in vitro* cardiac differentiation. Further, we optimized this model for screening cytokines/small molecules for their ability to enhance MESP1-progenitor proliferation. We further discuss future development of automated analysis of cell proliferation, using the eGFP-Anillin reporter, and we indicate its potential in the development of cardiomyocyte-proliferation assays, which will be of interest for the fields of regenerative medicine and assay development for drug discovery and toxicity[12-15].

METHODS

Lentiviral transductions in hESCs

To generate the hESC proliferation reporter line, 100k MESP1$^{w/mCherry}$ hESCs[4] were transfected with a lentiviral construct containing a CAG–eGFP–anillin expression cassette (0.5uL / 20k cells), and plated on a Matrigel (BD Biosciences; growth factor reduced, phenol red–free)-coated 24 wells plate (Falcon)[11]. Three days after transduction, hESCs were enzymatically passaged using 1x TrypLE Select (Life Technologies). After dissociation, cells were stained with anti-SSEA-4 in order to select for pluripotent hESCs, followed by resuspension in FACS sorting buffer (PBS with 0.5% BSA and 2.5mM EDTA) and filtration through a 40-µm cell strainer (Falcon). Cells were sorted using a BD ARIA III flow cytometer into 96 wells flat bottom low attachment plates. Live cells were gated on the basis of side scatter, forward scatter, anti-SSEA-4-PE, and eGFP-Anillin fluorescency. Flow cytometric gates were set using control cells labelled with the appropriate isotype control antibody.

Clone Selection and Culture

Due to the integration properties of lentiviral particles, five undifferentiated transfected clones were analysed for their eGFP-Anillin expression. Clone A4 and C6 were selected, based on their eGFP expression intensity, and further cultured as single cells on mouse embryonic fibroblasts on 9.96 cm2 6 well format (Falcon), in 3 mL hESC medium (DMEM F12, Non Essential Amino Acids, Knock Out Serum (Gibco by Life Technologies); bFGF (Miltenyi Biotec)) and were enzymatically passaged. hESCs from clones A4 and C6 were analysed for eGFP-Anillin expression. Clone A4 showed a more consistent and robust eGFP-Anillin expression and further experiments were performed with this clone.

Cardiac Differentiation

One day before differentiation, 10k hESCs were passaged onto a 96-well tissue culture dish (96 Well Optical CVG, ThermoScientific), coated with Matrigel (BD Biosciences) in 100uL of hESC medium per well. On the first day of differentiation, day 0, hESC medium was replaced by low insulin serum-free medium BPEL (BSA, polyvinyl alcohol, essential lipids, as previously described)[17, 24], containing the cytokines BMP4 (20 ng ml−1, R&D Systems) and Activin A (20 ngml−1, Miltenyi Biotec), and Chir99021 (1.5uM, AxonMedchem). At day 3 of differentiation, the medium was refreshed with BPEL containing 5uM Xav939 (R&D). To study their proliferation, we sorted MESP1-mCherry progenitors at day 2 of differentiation. Cells were plated back as monolayers in 96 wells plates (96 Well Optical CVG, ThermoScientific), in a density of 50k cells per well, in BPEL with 5uM Xav939 from day 2 until day 7.

Growth Factor Screening

For the *in vitro* growth factor screening, cells were differentiated as described before, on 96 well tissue culture dishes (Falcon). A complete list of the compounds used for screening, and the concentrations used, can be found in **Supplemental Table 1**. Growth factors were added to the cell culture at day 2 or day 3 of differentiation. The proliferative effect was assayed on day 4 of differentiation using a MACS Quant VYB flow cytometer (Miltenyi Biotec). The percentage of MESP1-mCherry+ cells was assessed for each treatment, and compared to control cells without treatment. Each experiment was performed in quadruplicate, and one or two independent experiments were performed for each condition.

Flow Cytometry

During cardiac differentiation, eGFP-Anillin and MESP1-mCherry expression were analysed every 24 hours. For this, cells were enzymatically dissociated using 1x TrypLE Select (Life Technologies). After dissociation, cells were resuspended in FACS sorting buffer (PBS with 0.5% BSA and 2.5mM EDTA) and analysed using a MACS Quant VYB flow cytometer (Miltenyi Biotec) and FlowJo Software with a 488 nm and a 561 nm laser. Co-expression of eGFP-Anillin with proliferation marker Ki-67 was analysed by flow cytometry in undifferentiated hESCs, and at differentiation day 3 and day 5. For this, dissociated cells were treated with FIX & PERM® Cell Fixation and Permeabilization Kit (Life Technologies) and stained with anti-Ki-67-PE (Biolegend).

Immunohistochemistry

eGFP-Anillin transduced MESP1-mCherry-cells were analyzed by immunohistochemistry (IHC) when undifferentiated, and at day 3, and 5 of differentiation. For this, cells were fixed in 2% PFA and stained for Ki-67 (MIB-1 M7240, DAKO (1:400)), PHH3 (Ser 10, Millipore 06-570 (1:100)), and aurora B kinase (SIGMA A5102 (1:200)). Primary antibodies were diluted in 0.2% TritonX in PBS, supplemented with 5% Donkey serum and incubated with the cells for 1.5 hour at room temperature (RT). Then, cells were washed 3x 5 minutes with PBS. The 2nd antibodies (mouse and rabbit Cy5 Jackson Immuno Research) were directly diluted (1:400) in Hoechst 33342 solution (1 µg/ml) in PBS and incubated for 1 hour at RT in dark. Then, cells were washed 3x with PBS and embedded in FLUKA mounting medium (Sigma10981) on glass-cover slips.

Statistical Methods

A two-tailed Student's T test was performed using Graphpad Prism software (Graphpad Software, La Jolla, CA, USA). Results were considered significant at P values <0.05.

Time Lapse Microscopy

In order to study cellular dynamics of MESP1 progenitors, eGFP-Anillin-MESP1$^{w/mCherry}$ hESCs were differentiated as previously described, and sorted at day 3 of differentiation. 50k cells were replated as monolayer onto a 96-well glass bottom plate (Thermo Scientific), coated with Matrigel. The cells were incubated on a stage-heated fluorescence image acquisition station (Leica AF6000). The plate was covered with a CO2 environment cover glass, supplied with 8% CO2/O2 inflow to maintain pH balance. Time-lapse imaging was started 5 hours after plating. Imaging settings can be found in supplemental table 2 (**Supp. Table 2**). Cell tracking was performed manually using the Fiji ImageJ plugin MTrackJ (E. Meijering, Methods in Enzymology 2012).

Automated Quantification of Proliferation

The pipeline of automated quantification of eGFP-Anillin localizations at single cell level contains two major parts: image analysis and data analysis. Image analysis procedure basically converts raw microscope images into quantified measurements representing characteristic biological phenomena. Three steps are elaborated to achieve this purpose: (1) image enhancement, (2) image segmentation and (3) phenotype measurement. Here, image enhancement aims at providing a better input for image segmentation by a list of techniques including background correction, noise suppression and contrast enhancement. Image segmentation partitions an image into multiple regions (single cell regions) with the goal to simplify the representation of an image into comprehensive components. For fluorescence

microscopy cell imaging, we utilized seeded propagation cell segmentation method[16]. The method segments the single nuclei using watershed segmentation based on Euclidian distance map (EDM) from the DAPI channel. The segmented single nuclei mask is treated as seed and propagate to find the Anillin positive cell area in the GFP channel. Phenotype measurements including shape and texture features are calculated on both individual nuclei and Anillin positive cell area masks. These phenotype measurements are further used as feature dataset in the data analysis part. In order to quantify the number of dividing cells versus non-dividing cells, a classifier was trained to distinguish the dividing cells from the image. Supervised classification strategy, which is based on ground truth analysis (dividing = 1 versus non-dividing = 0), was used in this study. First, a feature dataset was normalized in order to equalize the ranges of the features.

Second, the feature selection procedure was applied to select a subset of relevant features. Four representative feature selection methods were evaluated: the best individual-N features, the branch and bound procedure, greedy forward selection and greedy backward elimination[17]. Third, four classifiers covering both linear and non-linear categories; i.e. the linear classifier (LDC), the quadratic classifier (QDC), k-nearest neighbour classifier (KNNC) and support vector machine (SVC) were included for the classification evaluation. The final performance of the automated analysis was evaluated using the precision, recall and F-score[16, 18].

RESULTS

eGFP–Anillin expression marks proliferating hESCs.

In order to study the proliferative capacity of early pre-cardiac MESP1-mCherry progenitors, we transduced previously generated MESP1$^{w/mCherry}$ hESCs[4] with lentiviral particles containing a CAG-eGFP-Anillin fusion cassette[11], resulting in random genomic integration of the CAG-eGFP-Anillin reporter in actively transcribed genes (**Fig. 2**). Five targeted clones were obtained (showing the brightest eGFP expression in undifferentiated hESCs), from which clone A4 showed the most consistent expression (**Fig 3a**). In clone A4, eGFP-Anillin expression was analyzed for its co-expression with M-phase marker PHH3, proliferation marker Ki-67 (S, G1, G2, M phase), and aurora B (midbody expression) (**Fig 3b,c**). Indeed, we found correlating expression patterns of eGFP-Anillin with PHH3, aurora B co-expression with eGFP-Anillin in the midbody of dividing cells (telophase), and all cells positive for both eGFP-Anillin and Ki-67, indicating how different eGFP-Anillin localizations can distinct specific cell cycle stages from eachother.

eGFP-Anillin expression intensity decreases upon cardiac differentiation

To further characterize the MESP1$^{w/mCherry}$ eGFP-Anillin reporter, we differentiated cells (clone A4) as described before. We analyzed eGFP and mCherry expression every 24 hours from day 0 until day 5 of differentiation (**Fig. 4**). We found MESP1-mCherry levels peaking around day 2 and day 3 (12-14%). Furthermore, we observed all cells being positive for eGFP when in undifferentiated state, up to day 2 of differentiation. However, we found a rapid decrease in eGFP-Anillin intensity upon day 3 of differentiation, where we could only detect 75% of cells still positive for eGFP-Anillin. These levels decreased to only 37% at day 5 of differentiation, indicating cells entering the G0-phase upon differentiation. An alternative explanation for decreased expression of GFP can also attributed to epigenetic silencing of the transgene (for example by DNA-methylation and chromatin remodelling). To further investigate this, we performed analysis on Ki-67 co-expression at day 3 and day 5 of differentiation and compared this to eGFP-Anillin (**Fig. 5a,b**). Despite decreasing levels of eGFP-Anillin, we could still detect maintained expression of Ki-67 in a large population of cells (±80% at day3, and ±77% at day 5), indicating silencing of the construct upon differentiation at day 5. Moreover, at day 5 of differentiation, we could identify cells positively stained for Ki-67, and negative for Anillin-eGFP (**Fig. 5b**). The same image shows high variability of eGFP levels between cells, at both day 3 and 5 of differentiation. Based on these results we concluded that from day 5 onwards silencing of the transgene would interfere with the experimental outcome. Therefore, time-lapse imaging and analysis was performed up to day 4 of cardiomyocyte differentiation.

Proliferation of Early Cardiac Progenitors

In order to get insight in the proliferative capacity of early cardiac progenitors *in vitro*, we manually analysed cell division in the first four days of differentiation (**Fig. 6a**). Based the number of cells that was expressing eGFP-Anillin in the cytoplasm, cytoplasmic ring, and midbody region, the percentage of proliferating hESCs was measured to be approximately 4%, which was similar to the findings observed by Hesse et al.[11]. This proliferative capacity was largely decreased upon the first days of differentiation, and slightly increased after the formation of mesoderm (day 3,4). MESP1 progenitor division could be nicely visualized through the co-expression of mCherry with eGFP-Anillin localizations in the cytoplasm, cytoskeleton, and midbody. Moreover, dividing cells became rounded and were less spread out. They showed to have a proliferative capacity of about 2-3%, with no significant difference between early (day 2) and late (day 4) progenitors (**Fig 6a,b**). In order to get more insight in the proliferative capacity of MESP1-mCherry progenitors at single cell level, we performed time lapse imaging during cardiac monolayer differentiations, and of sorted MESP1-mCherry progenitors.

Induction of MESP1-mCherry proliferation

To identify signalling pathways involved in early cardiac progenitor proliferation, MESP1-mCherry–eGFP-Anillin hESCs were differentiated as described before and treated with growth factors/small molecules on day 2 or day 3 of differentiation. As a preliminary screen we measured the yield of MESP1-mCherry+ cells by automated flow cytometry, at day 4 of

differentiation (**Fig 7**). The control treatment did not contain any GFs (plain BPEL). For all growth factors we have added in our screening, we could not find a significant upregulation of mCherry+ cells, compared to control, indicating no aberrant role for these pathways in MESP1-progenitor proliferation under the tested conditions, which is in contrast to their role in proliferation of other early cardiac progenitors[6, 9, 19]. Therefore, we postulate that a complex combination and concentration of growth factors and possibly specific ECM components, which are highly expressed by MESP1-mCherry progenitors[4], may be required.

Real time tracking of MESP1-mCherry progenitors

In order to study the proliferative capacity of CPCs at single cell level, we developed a live single cell tracking system during differentiating, to follow division and migration of single cell MESP-mCherry expressing progenitors. For this, optimization of culture conditions and technical settings were required, which included light intensity of the fluorescent lamp, exposure time, autofocusing, heating temperature, objective magnification and objective immersion medium (**Supp. Table 2**). To decrease the effects of photo-bleaching, we used a low lamp intensity (4.3) and 2x2 binning (**Fig. 8a**). Another setting that required optimization included Z-position stability, or focal drift. Without autofocus, focal drift would occur, which makes long time-lapse experiment impossible. Since eGFP-Anillin signal diminishes easily, autofocus was set up in the bright field-DIC channel. This resulted in a consistent error in the focal plane of 5-6 µM, which was compensated by making images in multiple Z-planes.
In order to generate an assay to study the proliferative capacity of MESP1 progenitors live, we sorted MESP1-mcherry progenitors at day 3 of differentiation and replated them as monolayers at 96 wells plates with glass bottom. We started live-image acquisition after cell attachment (about 5 hours later). We used a maximum interval time of 10 minutes to be able to track single cells (**Fig. 8b**). Live cell division could be followed through the distinct localizations of the eGFP-Anillin reporter protein (**Fig. 8c**). We identified how the nucleus changes from oval to a more U-shaped form prior to cell division, and how cell shape became more rounded when eGFP-Anillin moved to the cytoplasm during the prophase. These changes prior to cell division are described as mitotic cell rounding. This was followed by the formation of a cytoplasmic ring, and a midbody upon cytokinesis. We estimated that the M-phase of early cardiac progenitors would take about 30 minutes, which is consistent with previous findings from Hesse et al. who demonstrated a similar time for the M-phase of hPSCs[11]. In a similar sort-and-replate experiment, we determined the migrating behaviour of MESP1-mCherry expressing progenitors, using a time interval of 15 minutes (**Fig. 8d**). We were able to follow MESP1-mCherry progenitors for up to 15 hours after replating and attachment (20 hours after sorting). Some tracked cells were lost, as they migrated out of focus. Further, we showed the ability to visualize MESP1-mCherry progenitor proliferation, and identified the distinct eGFP-anillin localizations marking the different stages of the M-phase and final cytokinesis (**Fig. 8e**).

To understand the dynamics of MESP1-mCherry progenitor proliferation and their further differentiation towards cardiomyocytes, it will be of interest to follow their behaviour and phenotype changes in time, through time lapse imaging at single cell level. Here, we show how sorted and replated MESP1-mCherry progenitors, were further differentiating over time, followed for up to 48 hours (**Fig. 9**). Bright MESP1 expression at day 3 was diminished upon further differentiation, and cell shape and behaviour changes could be observed. eGFP-anillin signal faded alongside MESP1-mCherry signal and was completely gone at day 5 of differentiation, possibly due to silencing upon differentiation (**Fig. 9**).

Automated Quantification of Proliferation

In order to study whether small molecules/growth factors may enhance proliferation of cardiac progenitors and/or cardiomyocytes using the eGFP-Anillin cassette, we developed a pipeline for automated quantification of eGFP-Anillin localizations at single cell level. For the image analysis part, we used a seeded propagation cell segmentation method to identify the single cells from the image. The precision of seeds (single nucleus) picking is crucial for a correct propagation procedure. The EDM watershed segmentation method works best for smooth convex objects that don't overlap too much. However, in our case, when cells are dividing, the shape of nuclei becomes irregular and dispersed. Furthermore, highly overlapping nuclei regions were observed in our image dataset. Therefore, we introduced a merging criterion which is based on the homogeneity of region intensity for the over segmented regions of nuclei under division. Since the number of highly overlapped nucleus regions is limited, these regions were excluded for the phenotype measurement. An example of the final segmentation result is shown in **Figure 10**. For the data analysis, 1500 individual cells (291 dividing cells and 1209 non-dividing cells) and 44 features were firstly collected as training dataset. During the classifier training, each combination of a feature selection method and a classifier algorithm was repeated for 100 times and the performance for each combination was evaluated using weighted classification error, which assigns different importance to different classes (www.mathworks.com)[20].
Based on this, we found that the combination of branch and bound feature selection (B&B) with k-nearest neighbour classifier (KNNC) has the lowest minimal value of mean weighted error and relatively small standard deviation of mean, as can be concluded from **Table 1**. The minimal value was reached when the feature selection method selects 4 features. These 4 features include smoothness of cell intensity, area of eGFP-Anillin positive cell area region, entropy of eGFP-Anillin signal in nuclei region, standard deviation of nuclei intensity.
Next, to identify the degree of errors in the automated analysis, we compared the results from manually quantifications of 22 images with their automated quantified counterpart as shown in **Figure 11a-d**. To demonstrate quantitatively the accuracy of the automated classification, we have used the Precision, Recall, and F-score metrics[21] **(Fig. 11e**). We reached a F-score equalling ±0.85, which meets or exceeds the performance of previous cell segmentation and/or pattern recognition studies[16, 22].

DISCUSSION

The availability of large numbers of cardiac committed progenitor populations is of high interest for translational purposes, such as cell therapy or drug discovery. An additional advantage is that it may provide us with a model for studying cardiac progenitor cells in relation to heart development. Although numerous studies have been conducted to unravel molecular and morphological aspects of heart development, in-depth knowledge regarding formation, proliferation, (subtype) differentiation and self-renewal of cardiac progenitors is limited. From *in vivo* mouse embryo studies it is evident that during gastrulation, cells ingress through the primitive streak and start to express mesendodermal transcription factors, including Brachyury T and Eomesodermin. From these cells, a posterior subpopulation develops that expresses key cardiac transcription factor MESP1. Lineage tracing studies in mouse have shown that the vast majority of the cells of the heart are derived from this MESP1-expressing population. In order to study the characteristics of these early pre-cardiac progenitor population in human, we previously developed a dual cardiac reporter MESP1$^{mCherry/w}$NKX-2-5$^{eGFP/w}$ hESC line[4]. This allowed us to isolate MESP1-mCherry expressing progenitors and to follow their further differentiation towards NKX2-5-eGFP expressing cardiac cells. In our current study, we were interested in the proliferative capacity of these MESP1 progenitors, in order to understand their potential as an unlimited source of cardiac progenitors. Several methods for measuring cell proliferation exist, on fixed and living material. M-phase marker PHH3 and active cell cycle marker Ki-67 are commonly used for measuring proliferation at fixed time-points. However, both markers require fixation and staining of samples, and are not appropriate for quantifying live cell division. Moreover, they are not specifically marking cytokinesis, and therefore do not distinguish between endoreduplication and cell division[11]. To overcome these limitations we made use of an *in vitro* reporter system that was recently developed[11], using the scaffolding protein anillin fused to eGFP. Here, we transduced MESP1$^{mCherry/w}$NKX-2-5$^{eGFP/w}$ hESCs with lentiviral particles containing the CAG-eGFP-Anillin cassette, and thereby developed an *in vitro* system to study the proliferation of early cardiac progenitors, up to day 5 of differentiation. Since activation of NKX2-5-eGFP occurs at later stages during differentiation (~day 7 and later), GFP expression at early stages could be attributed to Anillin-eGFP alone. In hESCs, we showed the different stages of the M-phase by distinct localizations of eGFP-Anillin, clearly discriminating cytokinesis from other cell cycle stages. We showed that the vast majority of eGFP-Anillin+ hESC co-localized with Ki-67 immunostaining, whereas dividing cells co-localized with PHH3. Upon differentiation of hESCs towards the cardiac lineage, we found decreasing eGFP levels, leading to absence of detectable GFP levels at day 6. One possible explanation for this decrease in GFP expression could be due to an increasing number of cells entering a quiescent cell cycle stage upon differentiation[23], although this is not very likely, since we only observed a slight decrease in Ki-67 levels during the first days of differentiation. A more plausible explanation is silencing of the gene in which the CAG-eGFP-Anillin cassette had integrated[24]. As the Anillin-eGFP signal could still be detected up to day 5 of differentiation, the generated reporter line allowed us to study early progenitor differentiation. By measuring at fixed timepoints, we found, that approximately 4% of undifferentiated hESCs were dividing. MESP1 progenitors show a similar percentage, with no difference between early (day 2) and late (day 4) MESP1 progenitors. To fully understand the proliferative capacity of MESP1 progenitors at single cell level, and to get insights into the dynamics of these progenitors prior their further differentiation towards cardiomyocytes, we decided to set up a time-lapse live imaging system. Many hurdles needed to be overcome, including photo bleaching of the fluorescent protein upon exposure to high light intensities, the ability to track migrating single cells (time interval of image acquisition, autofocus, and Z-stacks), and the amount of data generated from a long-term time-lapse study (3-5 days, 10 minute interval, 3 Z-stacks). Following optimization by adjusting these parameters we showed real-time tracking of MESP1-mCherry progenitors during proliferation and further differentiation. In future studies we will follow differentiation from day 0 up to day 5, where we will study the derivation of MESP1-mCherry expressing progenitors, and quantify their proliferative behaviour prior to their further differentiation towards cardiomyocytes. In addition, time lapse experiments at later stages of differentiation, in the previously developed MESP1$^{mCherry/w}$NKX-2-5$^{eGFP/w}$ hESC line, will be of interest to perform for a more complete understanding of the dynamics of MESP1 expressing progenitors and their further differentiation towards specific cardiac lineages. Moreover, time-lapse experiments on cell proliferation may also enlighten knowledge on circadian rythms of cardiac progenitors, for which evidence grows it is tightly regulating cellular function, such as proliferation and/or maturation[25].

For potential future high-throughput screening experiments on proliferation of cardiac progenitors or cardiomyocytes, we are currently working on the development of an automated quantification method using classifiers that are based on the distinct localizations of eGFP-Anillin. Using such an automated system, a large number of combinations of growth factors and small molecules can be screened for their enhancing effect on MESP1-progenitor proliferation. Our automated image analysis system is efficient to identify single cells from the image. However, segmentation of the nucleus with diverse morphology or in a highly overlapped region needs further improvement. Nevertheless, after selecting the most optimal automated classification method for our set-up, we managed to reach a high F-score equalling ±0.85, which exceeds the performance of previous cell segmentation studies. In further experiments, we will test our newly developed quantification method in the absence and presence of proliferation inhibitors and stimulators, to understand which improvements are desired for implementation of this method in large-scale screening experiments. Automated image analysis is a critical step for the development of phenotypic screens that allow high-speed, reproducible and quantitative analysis.

In order to identify crucial signalling pathways that play a role in cardiac progenitor proliferation, which would subsequently be of interest as target pathways in large-scale

screening experiments, pilot experiment were performed that included initial screenings on our standard monolayer differentiations. At day 2 or day 3 of differentiation, we removed the standard cardiac differentiation growth factors, and replaced them for potential growth-inductive cytokines. However, flow cytometry measurements after 24 hours of induction did not result in significant increased levels of MESP1-mCherry expressing progenitors. In contrast, previous findings showed that NKX2-5-progenitor proliferation could be enhanced by IGF-1 or in combination with SAG (a smoothened agonist), and SB431542 (TGF-β/Activin/Nodal inhibitor)[9, 19]. The lack of response in our assay may indicate that a combination of different factors is required for MESP1 progenitors to proliferate, and possibly in the presence of the right microenvironment, such as the specific composition of ECM proteins or other cell types[26].

Proliferation of cardiomyocytes in the human heart has been described, although the rate is very limited[27]. It is important to understand how, if any, factors may induce cardiomyocyte proliferation, which may have an impact on treatment of heart failure by regeneration of the damaged heart after infarction[12-15, 28, 29]. Further optimization and technical advancement of screening assays, such as the combination of an Anillin reporter with a cardiac reporter appropriate for live imaging and automated quantification may prove to be very useful for identifying molecules and their underlying mechanisms for specific differentiation and differentiation of cardiac cell- (sub)types, which may lead to new therapeutic strategies for the treatment of heart failure.

FIGURES

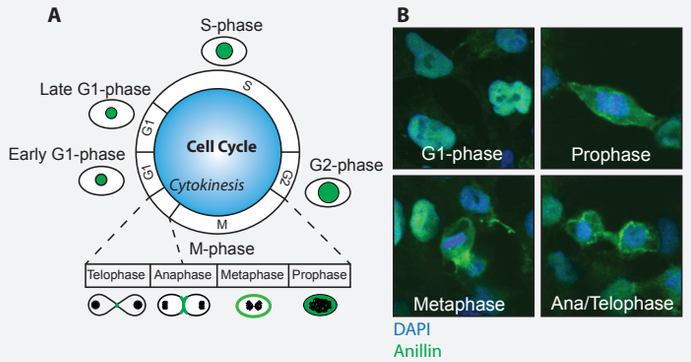

Figure 1. A: A schematic representation of Anillin. Localization of Anillin is visualized by fusion to eGFP and can be observed in the nucleus during G1-phase and migrates into the cytoplasm during prophase. During metaphase it appears in the cytoplasmic ring. Eventually, a midbody is formed during ana/telephase. Images are acquired using a 40x oil imm. Objective. *Figure 1a. is adapted from Hesse et al. Nature Communications 2011.* **B:** eGFP-Anillin localization in proliferating hESCs.

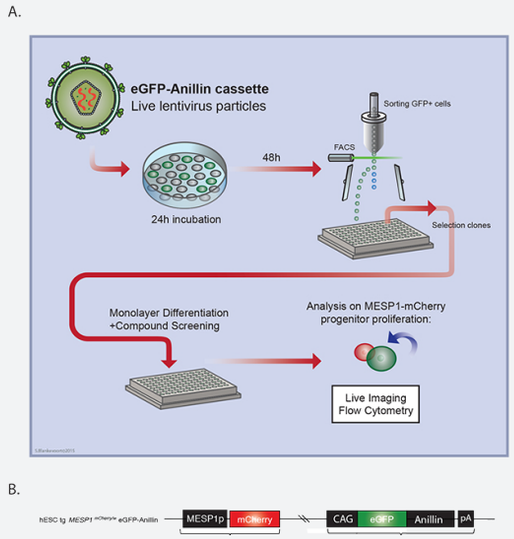

Figure 2. A: Overview scheme of how the eGFP-Anillin-MESP1mcherry/w reporter line was generated. hESCs were transfected with lentiviral particles containing the CAG-eGFP-Anillin cassette and were incubated for 24 hours. 48 hours after incubation, cells were sorted on eGFP expression and positive clones were selected for cardiac monolayer differentiations and compound screenings. Proliferation of MESP1-mCherry progenitors was assessed through live imaging of the eGFP-Anillin localizations**. B:** Schematic representation of the dual cardiac reporter line.

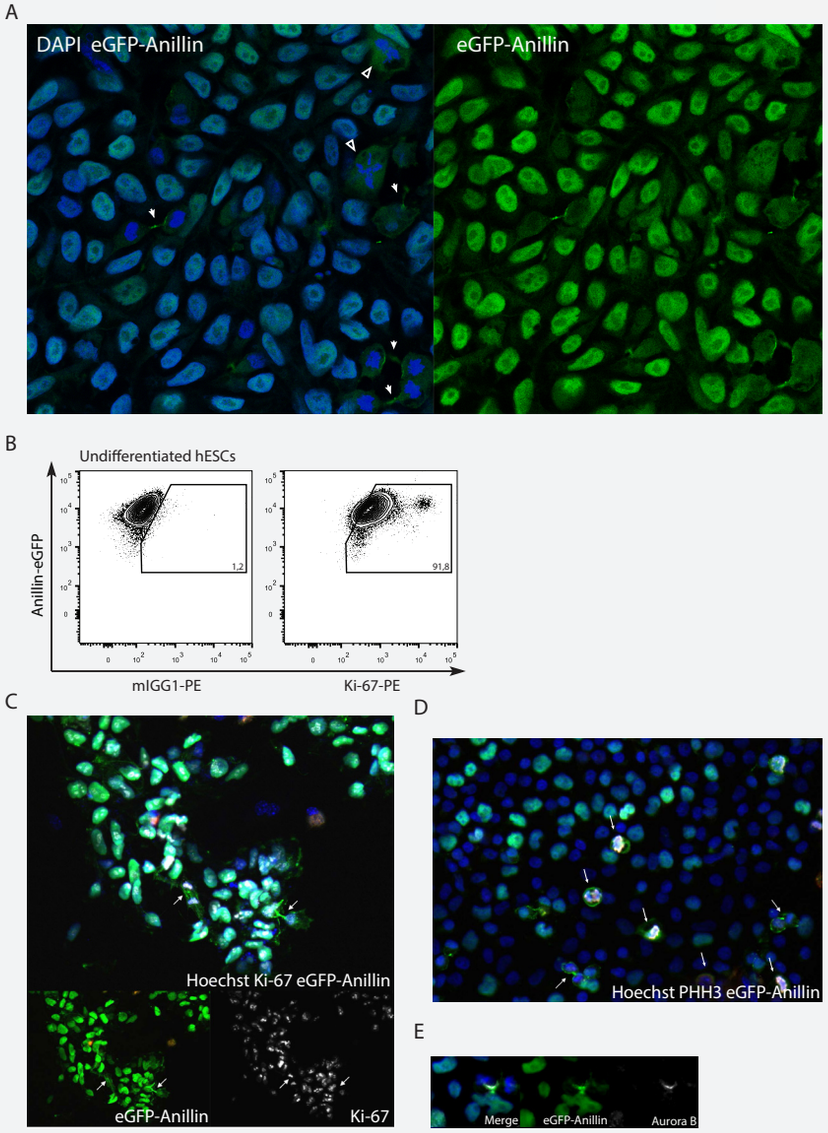

Figure 3. A: Picture of the dual reporter eGFP-Anillin-MESP1mcherry/w hESC line expressing eGFP–anillin under control of the CAG promoter. eGFP–Anillin (green) localization in the cytoplasm (open arrowhead), and midbody (arrow)**. B:** Flow cytometric analysis of eGFP-Anilin hESCs stained for Ki-67 (anti-Ki-67-PE) and control isotype (mIGG1-PE). **C,D,E:** Stainings for the proliferation markers PHH3 (red), Aurora B (grey), and Ki-67 (grey) reveals co-expression with the eGFP-Anillin signal (green). Nuclei are stained with Hoechst dye (blue).

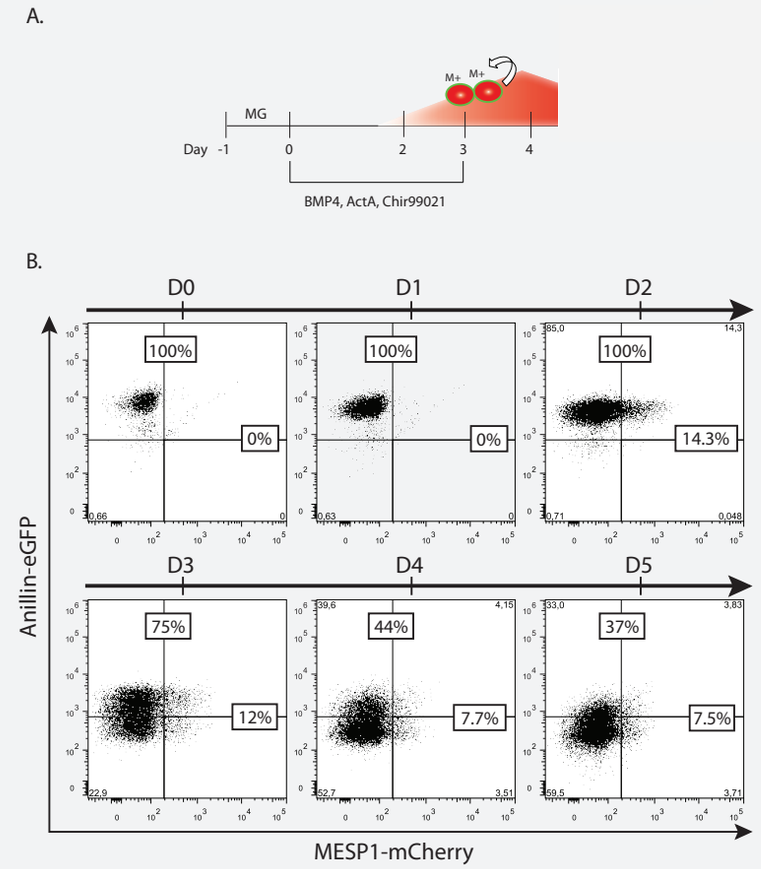

Figure 4. A: Cardiac monolayer differentiation protocol. MESP1-mCherry expression starts around day 2, and peaks between day 3 and day 4. Proliferation can be studied based on eGFP-Anillin expression. **B:** Flow cytometric analysis during cardiac differentiation, every 24 hours, from day 0 until day 5. eGFP-Anillin levels slowly decrease upon further differentiation.

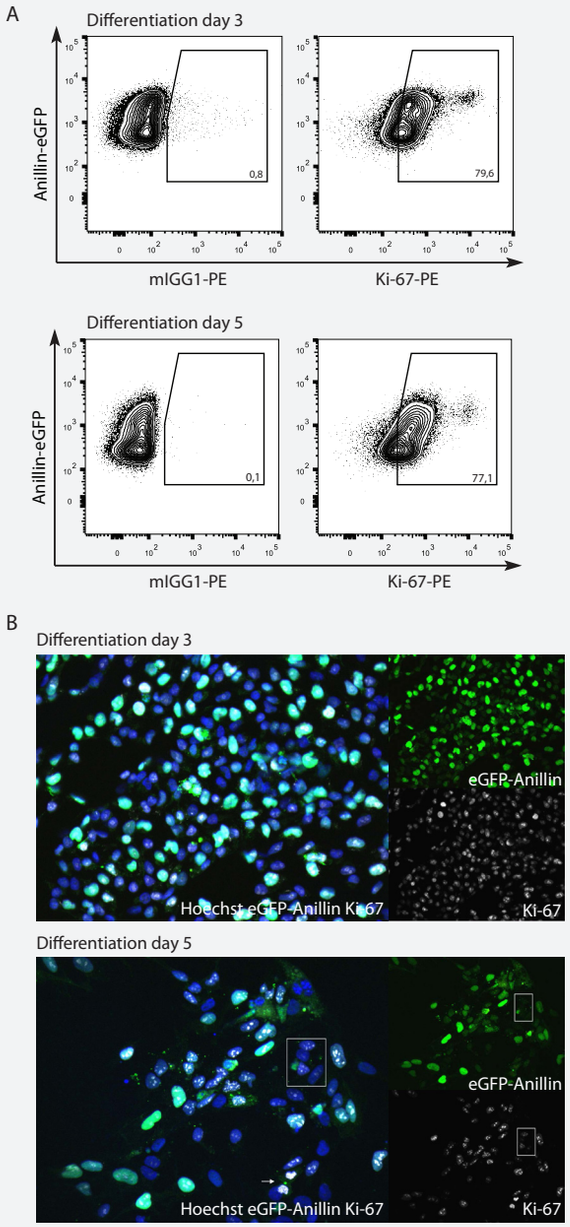

Figure 5. Flow cytometric analysis of Ki-67 co-expression with eGFP-Anillin- MESP1-mCherry expressing progenitors, at day 3 and day 5 of differentiation. Ki-67 levels remain high, despite a slight decrease, whereas eGFP-Anillin levels have decreased significantly, when compared to day 0 levels (Figure 4). **B:** Co-stainings for Ki-67 at day 3 and day 5 of differentiation revealed a large percentage of Ki-67 positive cells (active cell cycle) that show diminished eGFP-Anillin levels, indicating silencing of the construct.

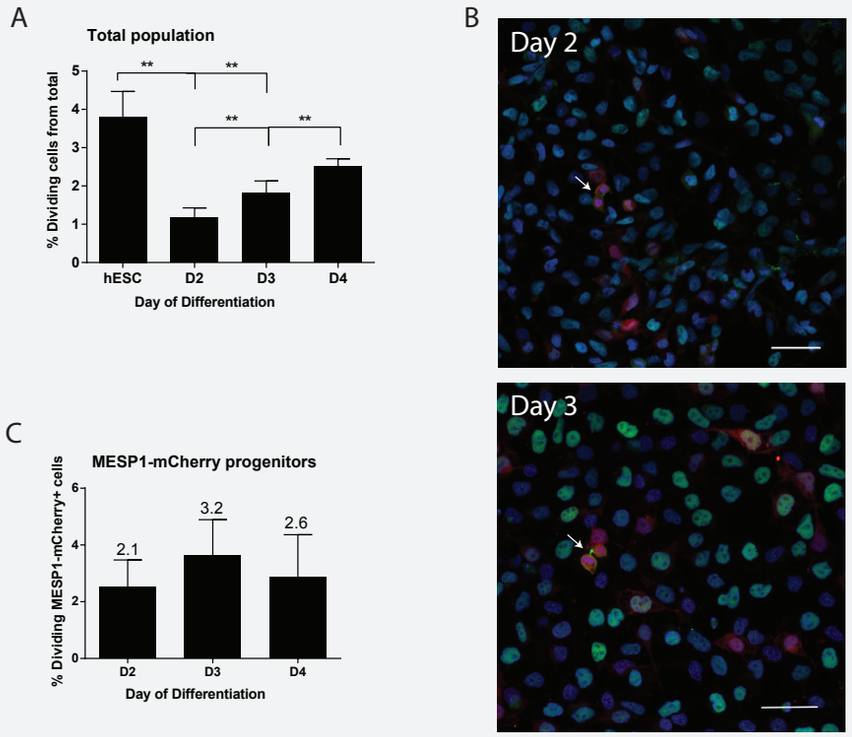

Figure 6. A: Percentage of all cells dividing (eGFP-Anillin M-phase localizations) upon early cardiac differentiation. **B:** Picture of a cardiac monolayer differentiation at day 3 visualizing proliferating (green) MESP1-mCherry progenitors (red). Nuclei are stained with DAPI (blue). **C:** Percentages of MESP1-mCherry progenitors dividing at day 2, day 3, and day 4 of differentiation. No significant differences between early and late progenitors were found. Scale day 2: 40uM. Scale day 3: 30uM.

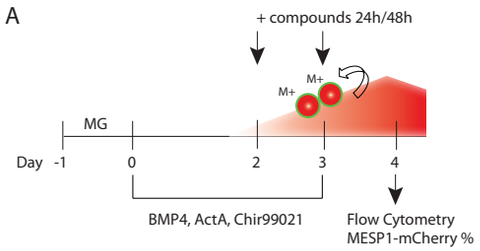

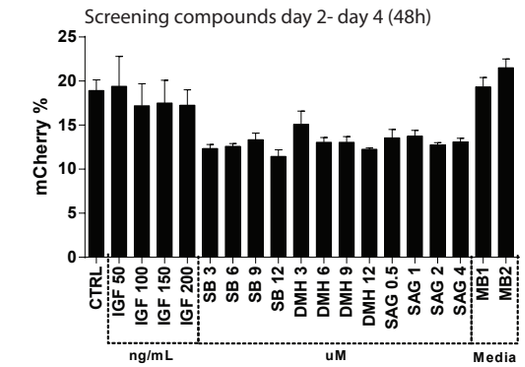

Media

MB1	Long R3 IGF-1	**MB2**	Long R3 IGF-1
	SAG		SAG
	SB431542		SB431542
	SU5402		bFGF
	DMH-1		BMP4
SH1	Long R3 IGF-1	**SH2**	FGF
	SU5402		BMP4
	DMH-1		Long R3 IGF-1
		CR	Chir
SH3	BMP4		DM
	Long R3 IGF-1		SB431542

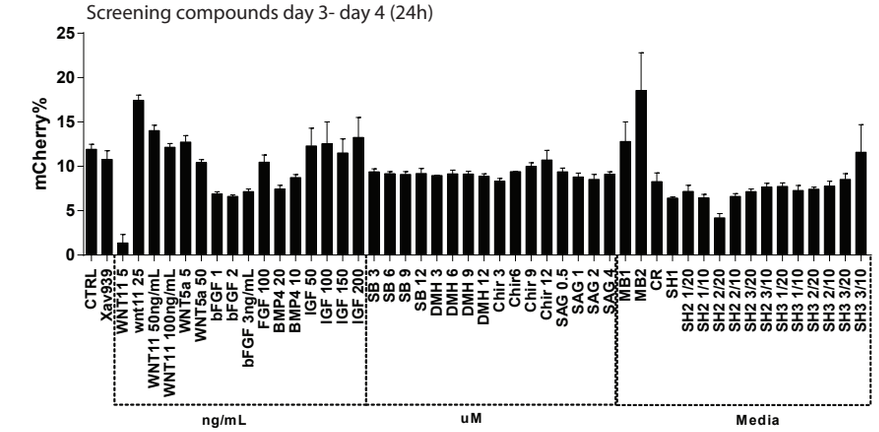

Figure 7. A: Schematic overview of proliferation compound screenings upon a monolayer cardiac differentiation. Cells were differentiated as described before. At day 2 or day 3, BMP4, Activin A, and Chir were removed, and replaced with screening compounds for 48 or 24 hours, respectively. At day 4 of differentiation, the percentage of MESP1-mCherry progenitors in the total population was measured by flow cytometry. **B,C:** Percentages of MESP1-mCherry progenitors measured by flow cytometry at day 4 of differentiation, after treatment with compounds for 24 or 48 hours. No significant differences could be identified, when compared with control treatment (no GFs).

A

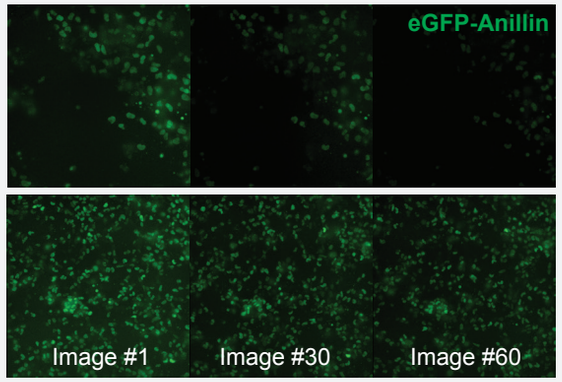

B: Cell Tracking on eGFP-Anillin signal

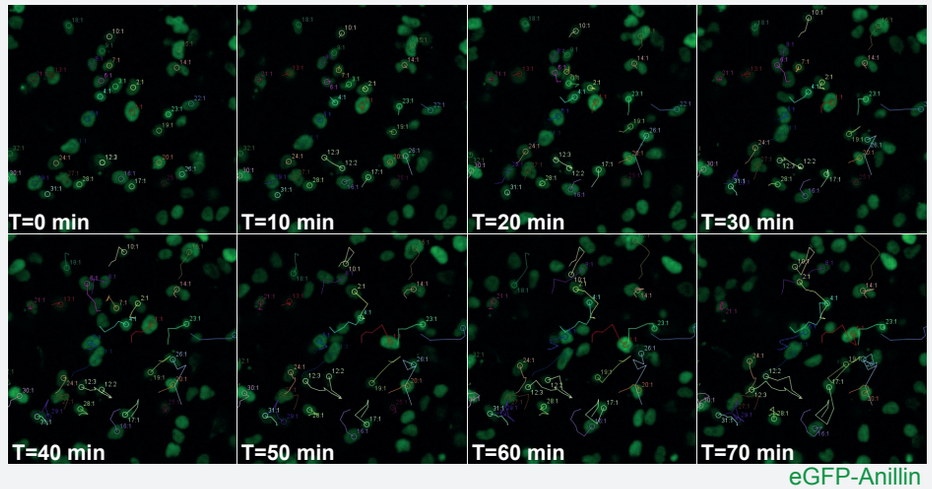

C: Live Cell Division

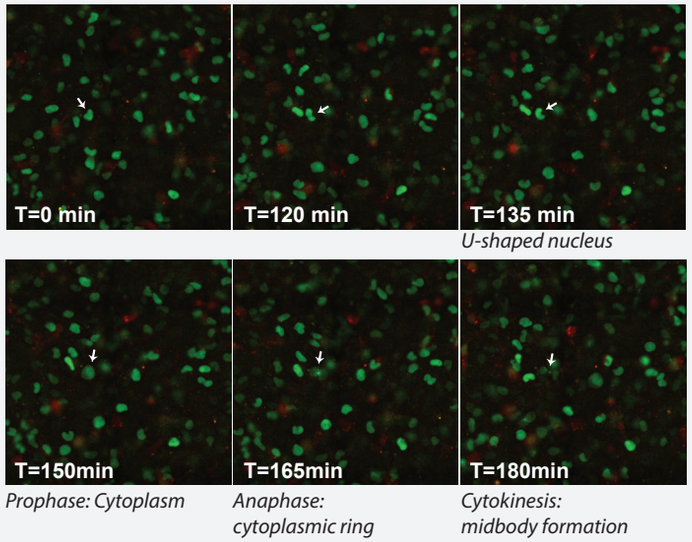

D: Cell Tracking of MESP1-mCherry expressing progenitors

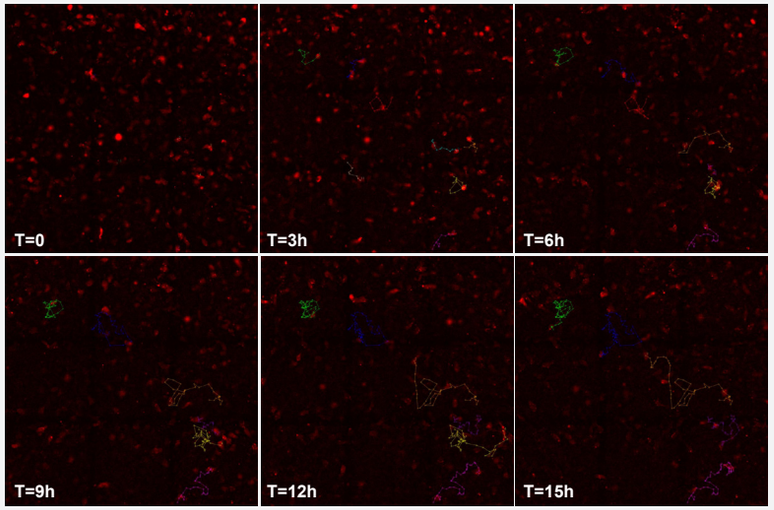

E: Live Cell Division of MESP1-mCherry expressing progenitors

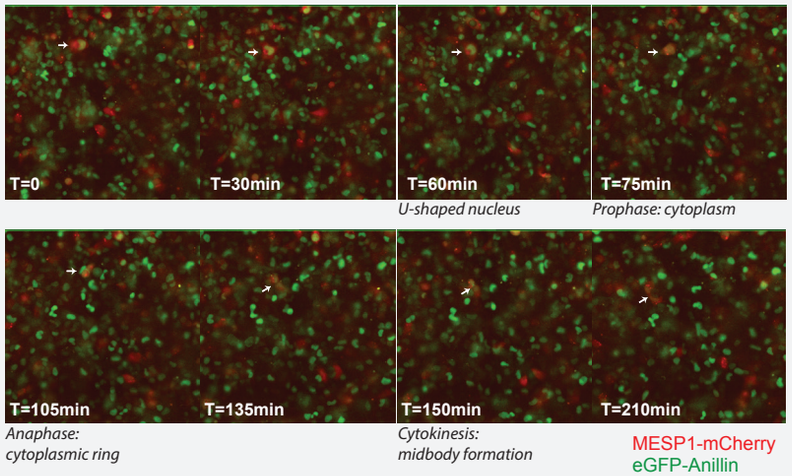

Figure 8: A: Settings for live-imaging fluorescent microscopy were optimized to prevent bleaching. 60 Sequential images were acquired with 63x glycerine immersion objective at minimised interval. The intensity of the lamp, exciting the fluorophores, is of great importance to prevent bleaching. By closing the lamp and microscope light shutter, the intensity of the light was reduced which resulted in decreased bleaching. **B**: A time interval of 10 minutes allows manual cell tracking of eGFP-Anillin expressing cells. **C.** Live visualization of dividing cell upon cardiac differentiation. A U-shaped nucleus is visible prior to cell division (arrow). Images are 2,5xzoom from original acquired image size. **C:** Manual tracking of MESP1-mCherry progenitors shows minimal migrative behaviour over a time span of 15 hours. Cell tracking stopped when cells were out of focus. Time interval of image acquisition: 15 minutes. **D:** Live visualization of dividing MESP1-mCherry progenitor (arrow). A U-shaped nucleus is visible prior to cell division. Images are 2,5xzoom from original acquired image size.

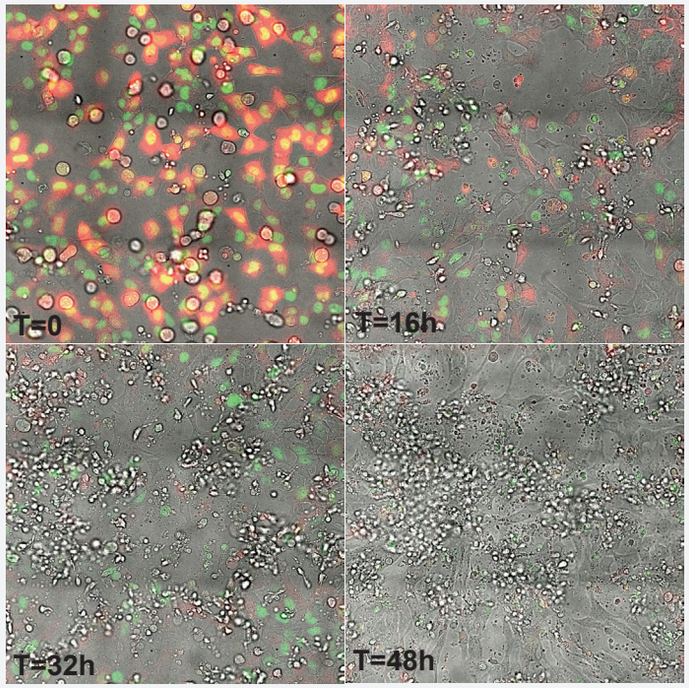

Figure 9. A: Time-lapse imaging of MESP1-mCherry sorted and replated progenitors. Images were acquired using a glycerol immersion 63x objective. T is given in minutes. To be able to track the highly migrative cells, a 10 minute interval was set. **B:** Time-lapse imaging of MESP1-mCherry sorted and replated progenitors. The Anillin-eGFP signal gets silenced upon further differentiation. mCherry levels decrease, as MESP1 levels are downregulated upon further differentiation. Morphological changes can be observed: cells become elongated and obtain a mesenchymal phenotype. T is given in hours.

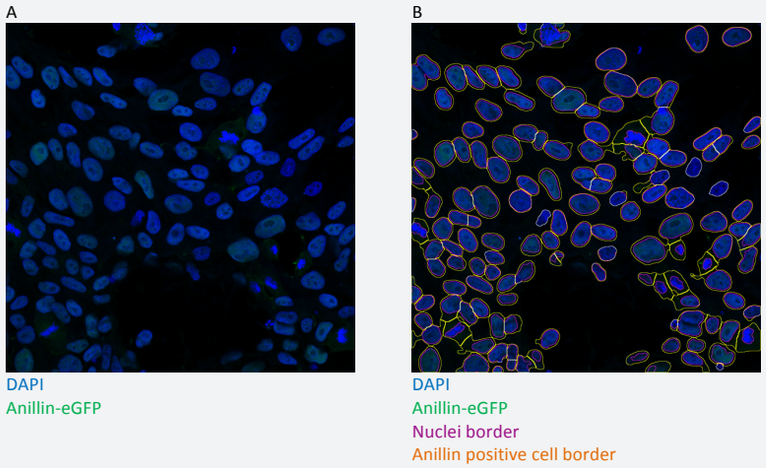

Figure 10. Automated Segmentation Result.

A

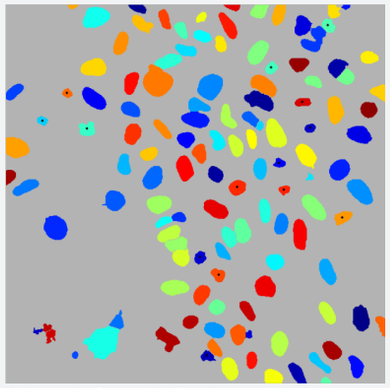

Automated annotation 1

B

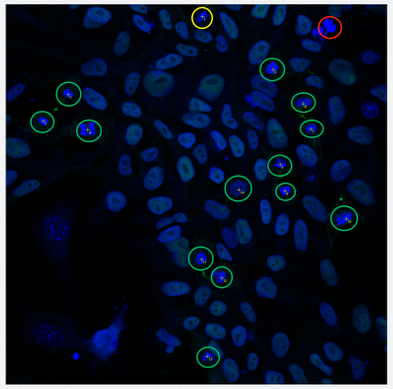

Manual annotation 1

C

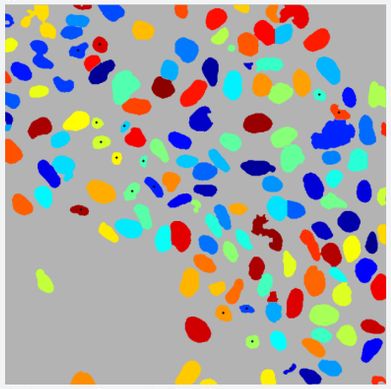

Automated annotation 2

D

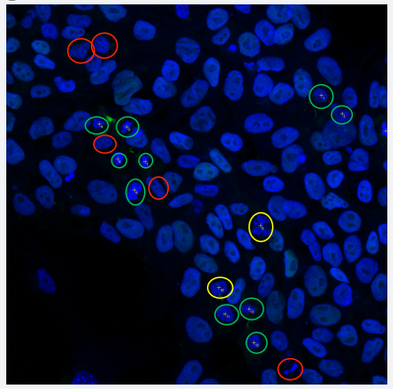

Manual annotation 2

E. Comparison of automated and manual cell segmentation by F-score analysis.

	TP:	TP + FP:	TP + FN:
Total:	399	490	444
	Precision:	**Recall:**	**F-score:**
	0,814285714	0,898648649	0,854389722

$$Precision = \frac{TP}{TP + FP}$$

$$Recall = \frac{TP}{TP + FN}$$

$$F\text{-}score = \frac{2PR}{P + R}$$

Figure 11. Automated Annotation versus Manual Annotation. To identify the degree of errors in the automated analysis, we compared the results from manually quantifications of 22 images with their automated quantified counterpart. **A-D:** Green circles: positive and selected. Yellow circles: false negative. Red circles: false positive. **E:** Calculation of F-score. TP: true positives. FP: false positives. FN: false negatives. P: Precision. R: Recall.

Weighted classification error: the sum of k-th class error divided by the k-th class size multiplying the weight k which is the prior probability of k-th class.

$$error_w = \sum_{k=1}^{i} w_k * (\frac{e_k}{n_k})$$

e_k is the number of misclassified training examples from the k-th class and n_k is the size of the k-th class in the training set.

Calculation of weighted classification error in this study:

$$error_w = \left(\frac{291}{1500}\right) * \frac{e_{div}}{n_{div}} + \left(\frac{1209}{1500}\right) * \frac{e_{non-div}}{n_{non-div}}$$

Minimal $error_w$ calculated for each feature selection method:

	Individual		B&B		Backward		Forward	
	min	sem	min	sem	min	sem	min	sem
LDC	0.0322	0.0014	0.0314	0.0013	0.0344	0.0013	0.0352	0.0012
QDC	0.0388	0.0017	0.0336	0.0014	0.0406	0.0014	0.0426	0.0013
KNNC	0.0359	0.0014	**0.0256**	0.0011	0.0317	0.0013	0.0320	0.0013
SVC	0.0355	0.0013	0.0285	0.0013	0.0314	0.0014	0.0313	0.0013

Individual: best individual N feature selection method; B&B: branch and bound feature selection method; Backward: greedy backward elimination method; Forward: greedy forward selection method; min: minimal value of mean weighted error; sem: standard error of mean; LDC: the linear classifier; QDC: the quadratic classifier; KNNC: the k-nearest neighbour classifier; SVC: support vector machine classifier. REFS: www.mathworks.com and Polo 1997.

Table 1. Minimal Value of Mean Weighted Errors for each Feature Selection Method.

Cytokine	Concentration
Long R3 IGF-1	50 ng/mL
	100 ng/mL
	150 ng/mL
	200 ng/mL
SB431542 (Tocris)	3 uM
	6 uM
	9 uM
	12 uM
Dorsomorphin	3 uM
Homologue-1	6 uM
(DMH)	9 uM
	12 uM
SAG (Millipore)	0.5 uM
	1 uM
	2 uM
	4 uM
Wnt11 (R&D)	5 ng/mL
	25 ng/mL
	50 ng/mL
	100 ng/mL
bFGF	1 ng/mL
	2 ng/mL
	3 ng/mL
	100 ng/mL
Wnt5a (Millipore)	5 ng/mL
	50 ng/mL
XAV939	5 uM

Medium	FGF (ng/mL)	BMP4 (ng/mL)	IGF
SH2	1	10	100 ng/mL
	2	10	100 ng/mL
	1	20	100 ng/mL
	2	20	100 ng/mL
	3	10	100 ng/mL
	3	10	100 ng/mL
SH3	1	10	-
	2	10	-
	1	20	-
	2	20	-
	3	10	-
	3	10	-

Medium	IGF	SAG (Millipore)	SB431542 (Tocris)	SU5402	DMH1	bFGF	BMP4
MB1	100 ng/mL	1 uM	5 uM	5 uM	0.5uM	-	-
MB2	100 ng/mL	1 uM	5 uM	-	-	1 ng/mL	20 ng/mL

Medium	Chir	DM	SB431542
CR	3 uM	2uM	0.5uM

Supplemental Table 1. Microscopy live imaging settings

Objective:	63x Glyc
Channels;	eGFP, mCherry and Brightfield
Image Interval:	10 minutes
Imaging Time:	64 hours
Z-Stack:	3x 5µM
Binning:	2x2
Autofocus:	Brightfield, compensated with zstack
Stitching:	3x3 (x: 59.6 y: 35.371)

Channels:	Exposure (ms)	EM gain	Intensity
eGFP	125	1100	4,3
mCherry (txred)	125	1100	4,3
Brightfield	30	1100	5

Supplemental Table 2. Small molecules/Growth factors screened

REFERENCES

1. Fuster V, Voute J, Hunn M, et al. Low priority of cardiovascular and chronic diseases on the global health agenda: a cause for concern. CIRCULATION … 2007;116(17):1966–1970.
2. Orlova VV, van den Hil FE, Petrus-Reurer S, et al. Generation, expansion and functional analysis of endothelial cells and pericytes derived from human pluripotent stem cells. NATURE PROTOCOLS 2014;9(6):1514–1531.
3. Burridge PW, Matsa E, Shukla P, et al. Chemically defined generation of human cardiomyocytes. NAT METH 2014:–.
4. Hartogh Den SC, Schreurs C, Monshouwer-Kloots JJ, et al. Dual Reporter MESP1 mCherry/w-NKX2-5 eGFP/whESCs Enable Studying Early Human Cardiac Differentiation. STEM CELLS 2014;33(1):56–67.
5. Elliott DA, Braam SR, Koutsis K, et al. NKX2-5eGFP/w hESCs for isolation of human cardiac progenitors and cardiomyocytes. NAT METH 2011;8(12):1037–1040.
6. Qyang Y, Martin-Puig S, Chiravuri M, et al. The Renewal and Differentiation of Isl1+ Cardiovascular Progenitors Are Controlled by a Wnt/β-Catenin Pathway. CELL STEM CELL 2007;1(2):165–179.
7. Engels MC, Rajarajan K, Feistritzer R, et al. IGF promotes cardiac lineage induction by selective expansion of cardiogenic mesoderm in vitro. EUROPEAN HEART JOURNAL 2013;34(suppl 1):P5037.
8. Kwon C, Qian L, Cheng P, et al. A regulatory pathway involving Notch1/β-catenin/Isl1 determines cardiac progenitor cell fate. NATURE CELL BIOLOGY 2009;11(8):951–957.
9. Birket MJ, Ribeiro MC, Verkerk AO, et al. Expansion and patterning of cardiovascular progenitors derived from human pluripotent stem cells. NATURE BIOTECHNOLOGY 2015;33(9):970–979.
10. Saga Y. MesP1 is expressed in the heart precursor cells and required for the formation of a single heart tube. DEVELOPMENT 1999:1–11.
11. Hesse M, Raulf A, Pilz G-A, et al. Direct visualization of cell division using high-resolution imaging of M-phase of the cell cycle. NAT COMMS 2012;3:1076.
12. Engel FB, Hsieh PCH, Lee RT, et al. FGF1/p38 MAP kinase inhibitor therapy induces cardiomyocyte mitosis, reduces scarring, and rescues function after myocardial infarction. PROC. NATL. ACAD. SCI. U.S.A. 2006;103(42):15546–15551.
13. Kühn B, del Monte F, Hajjar RJ, et al. Periostin induces proliferation of differentiated cardiomyocytes and promotes cardiac repair. NAT. MED. 2007;13(8):962–969.
14. Xin M, Olson EN, Bassel-Duby R. Mending broken hearts: cardiac development as a basis for adult heart regeneration and repair. NAT REV MOL CELL BIOL 2013;14(8):529–541.
15. Bersell K, Arab S, Haring B, et al. Neuregulin1/ErbB4 Signaling Induces Cardiomyocyte Proliferation and Repair of Heart Injury. CELL 2009;138(2):257–270.
16. Bass GT, Ryall KA, Katikapalli A, et al. Automated image analysis identifies signaling pathways regulating distinct signatures of cardiac myocyte hypertrophy. JOURNAL OF MOLECULAR AND … 2012.
17. Webb AR. Statistical Pattern Recognition - Andrew R. Webb - Google Books. 2003.
18. Ruusuvuori P, Äijö T, Chowdhury S. Evaluation of methods for detection of fluorescence labeled subcellular objects in microscope images. BMC … 2010.
19. Engels MC, Rajarajan K, Feistritzer R, et al. Insulin-Like Growth Factor Promotes Cardiac Lineage Induction In Vitro by Selective Expansion of Early Mesoderm. STEM CELLS 2014;32(6):1493–1502.
20. Juan J, Cubero C. Weighted Classification Using Decision Trees for Binary Classification Problems. LECTURE NOTES IN COMPUTER SCIENCE 1997.
21. Abdelsamea M, Mohamed MH, Bamatraf M. An Effective Image Feature Classiffication using an improved SOM. ARXIV 2015.
22. García-Olalla O, Alegre E, Fernández-Robles L, et al. Vitality Assessment of Boar Sperm Using an Adaptive LBP Based on Oriented Deviation. In: Computer Vision-ACCV ….Vol 7728. Lecture Notes in Computer Science. Berlin, Heidelberg: Springer Berlin Heidelberg; 2013:61–72.
23. Zavitz KH, Zipursky SL. Controlling cell proliferation in differentiating tissues: genetic analysis of negative regulators of G1-->S-phase progression. CURR. OPIN. CELL BIOL. 1997;9(6):773–781.
24. Xia X, Zhang Y, Zieth CR, et al. Transgenes Delivered by Lentiviral Vector are Suppressed in Human Embryonic Stem Cells in A Promoter-Dependent Manner. STEM CELLS AND DEVELOPMENT 2007;16(1):167–176.
25. Pre Du BC, Van Veen TAB, Young ME, et al. Circadian Rhythms in Cell Maturation. PHYSIOLOGY 2014;29(1):72–83.
26. Ieda M, Tsuchihashi T, Ivey KN, et al. Cardiac fibroblasts regulate myocardial proliferation through beta1 integrin signaling. DEVELOPMENTAL CELL 2009;16(2):233–244.
27. Bergmann O, Zdunek S, Felker A, et al. Dynamics of Cell Generation and Turnover in the Human Heart. CELL 2015;161(7):1566–1575.
28. Hartogh SCD, Sluijter JP, Doevendans PA, et al. Cellular Therapy for the Infarcted Myocardium. In: Translational …. Totowa, NJ: Humana Press; 2012:341–390.
29. Passier R, van Laake LW, Mummery CL. Stem-cell-based therapy and lessons from the heart. NATURE 2008;453(7193):322–329.